TEXAS
The University of Texas at Austin

COVID-19 Healthcare Demand Projections: 22 Texas Cities

Dr. Zhanwei Du, Xutong Wang, Remy Pasco, Michaela Petty, Dr. Spencer J. Fox, Dr. Lauren Ancel Meyers

CORRESPONDING AUTHOR
Lauren Ancel Meyers
The University of Texas at Austin
laurenmeyers@gmail.com

COVID-19 Healthcare Demand Projections: 22 Texas Cities

Dr. Zhanwei Du, Xutong Wang, Remy Pasco, Michaela Petty, Dr. Spencer J. Fox, Dr. Lauren Ancel Meyers

Corresponding author:
Lauren Ancel Meyers
The University of Texas at Austin
laurenmeyers@gmail.com

Overview

To support planning by cities across Texas, we analyzed all 22 Texas city modules of our *US COVID-19 Pandemic Model* to project the number of hospitalizations under four different social distancing scenarios. Note that the results presented herein are based on multiple assumptions about the transmission rate and age-specific severity of COVID-19. There is still much we do not understand about the transmission dynamics of this virus, including the extent of asymptomatic infection and transmission. We update our model inputs on a daily basis, as our understanding of the virus improves. Appendix 1 below provides our current estimates.

These results are not forecasts and do not represent the full range of uncertainty. Rather, they are meant to serve as plausible scenarios for gauging the likely impacts of social distancing measures in Texas cities.

We are sharing these results prior to peer review to provide intuition for policy makers regarding the immediate threat of COVID-19, the risks of medical surges, and the extent to which early social distancing measures can mitigate the threat. Our projections indicate that COVID-19 may quickly exceed healthcare capacity across Texas cities and that extensive social distancing measures can both delay and diminish pandemic surges.

COVID-19 projections for 22 Texas metros/cities with school closures and social distancing

We used our *US COVID-19 Pandemic Model* to simulate COVID-19 epidemics in 22 Texas cities and metropolitan areas. The simulations ran from April 1 through mid-August, 2020. They assume the following initial conditions and key parameters:

- Starting condition: Initialize simulations on April 1, 2020 assuming the total number of confirmed cases reported by counties in each city by that date (Table A2.1). For cities reporting zero cases, we assumed that one adult was infected on April 1, 2020. Given that many cases are likely not detected, we are likely underestimating the current prevalence of COVID-19. Thus, we made a second set of projections in which the number of initial cases on April 1, 2020 was set to ten times the cumulative confirmed cases.
- Epidemic doubling time: 4 days [1]
- Reproduction number: 2.2 [2]
- Average incubation period: 7.1 days [3]
- Proportion of cases asymptomatic: 17.9% [4]

All other model parameters, including age-specific hospitalization and fatality rates are provided in Appendix 1. The full structure and the Texas component of the US COVID-19 Pandemic Model are described in Appendix 2.

There are two sets of figures and tables below that summarize projections based on COVID-19 simulations for the 22 Texas cities.

- Base projections (Figures 1-5 and Table 1): simulations begin on April 1 assuming that the number of people infected is equal to the total number of confirmed reported cases in each city/MSA as of April 1 (Table A2.1).
- Adjusted projections (Figures 6-10 and Table 2): simulations begin with ten times the number of infected cases as the base case.

Base case

Figures 1-5 and Table 1 project COVID-19 cases, hospitalizations, ICU patients, ventilator requirements and deaths assuming that the number of people infected is equal to the total number of confirmed reported cases in each city/MSA as of April 1 ([Table A2.1](#)).

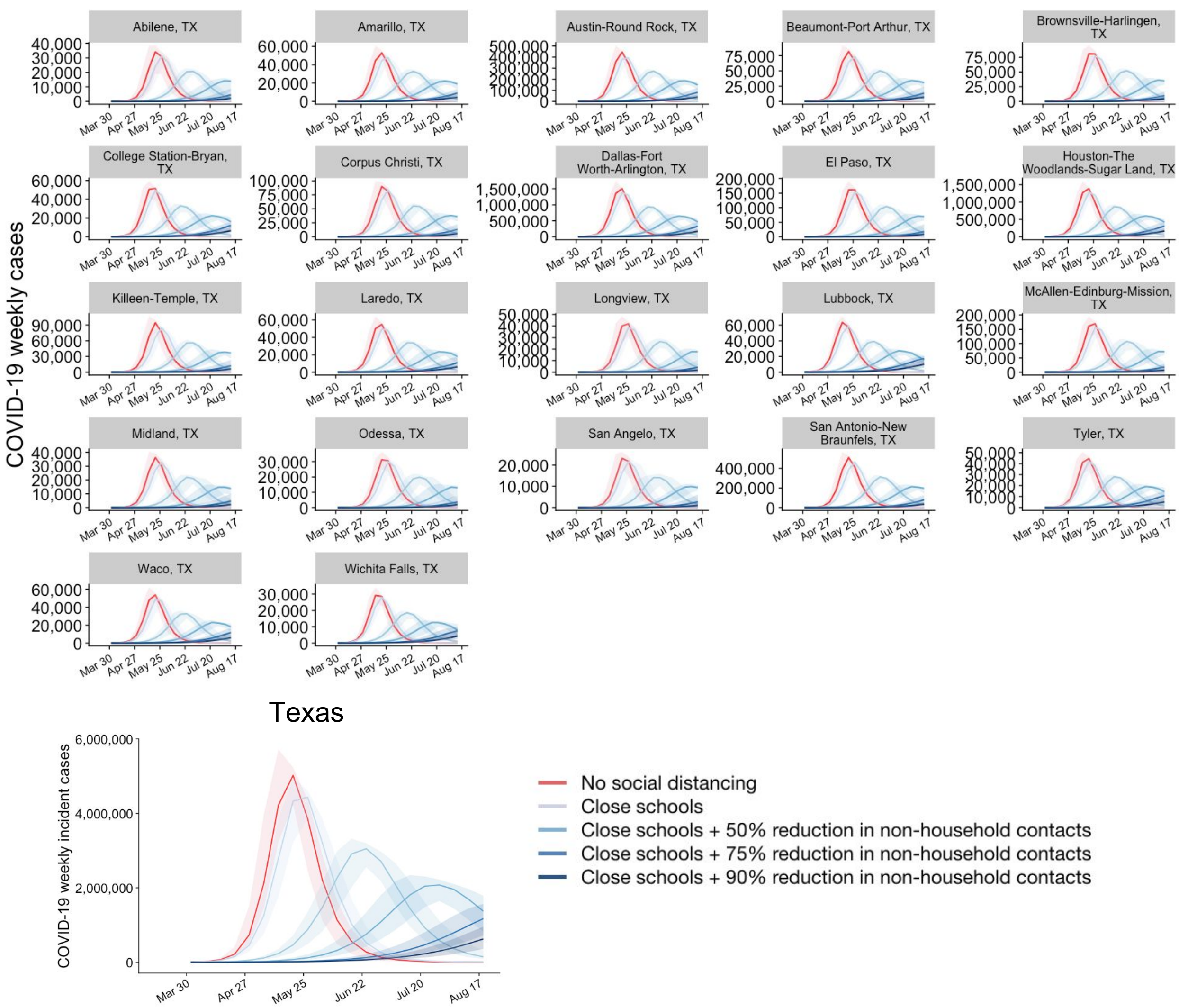

Figure 1. Projected new COVID-19 cases each week in 22 Texas metro/cities and summed across all 22 cities (bottom graph) under school closures from April 1 to August 17, 2020 coupled with different degrees of social distancing (starting from reported case counts on April 1). The red lines project COVID-19 transmission assuming no interventions. The blue lines show increasing levels of social distancing interventions, from light to dark: school closures plus social distancing interventions that reduce non-household contacts by either 50%, 75% or 90%. Lines and shading indicate the median value and interquartile range across 100 stochastic simulations.

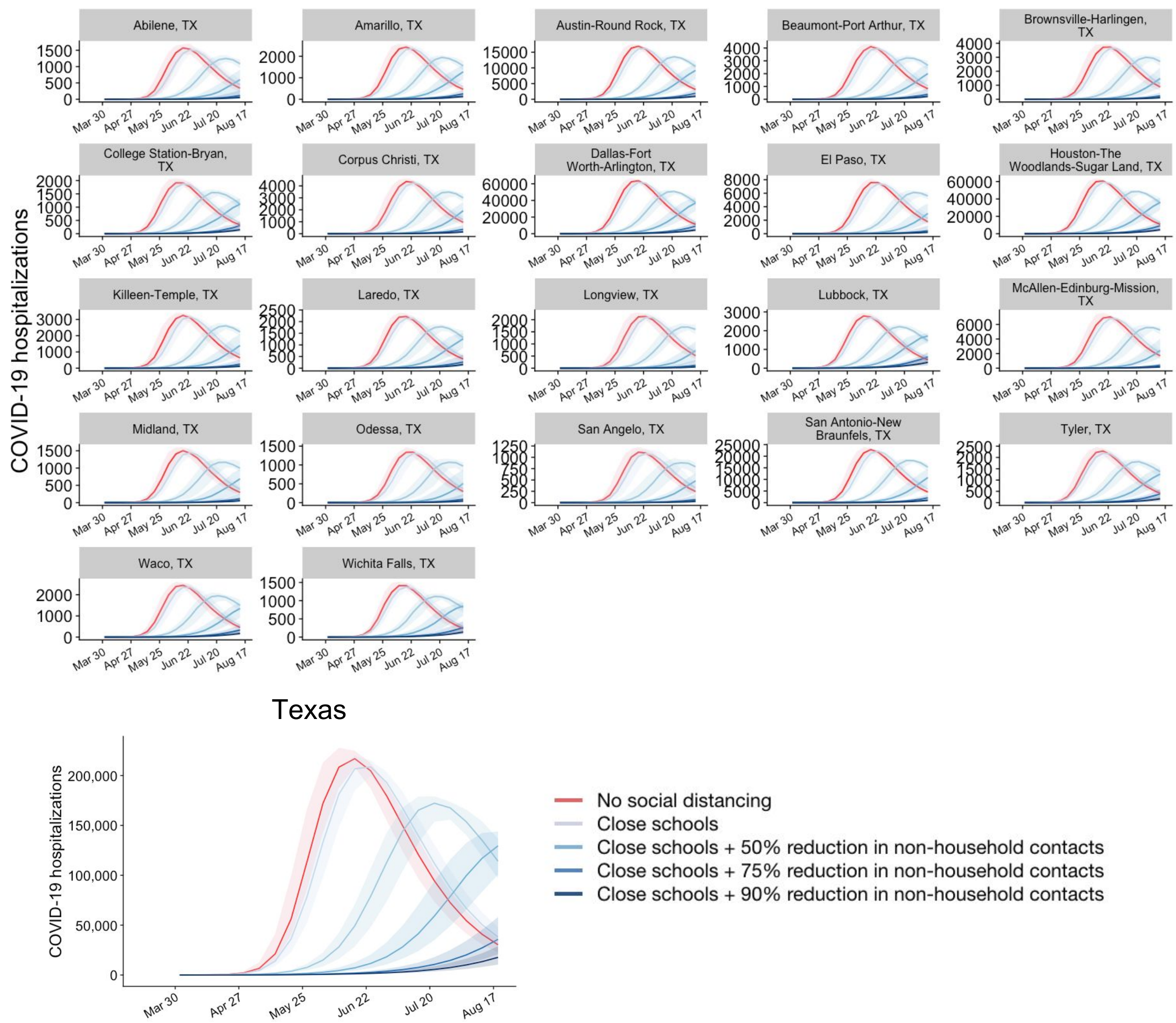

Figure 2. Projected COVID-19 hospitalizations in 22 Texas metro/cities and summed across all 22 cities (bottom graph) under school closures from April 1 to August 17, 2020 coupled with different degrees of social distancing (starting from reported case counts on April 1). The red lines project COVID-19 transmission assuming no interventions. The blue lines show increasing levels of social distancing interventions, from light to dark: school closures plus social distancing interventions that reduce non-household contacts by either 50%, 75% or 90%. Lines and shading indicate the median value and interquartile range across 100 stochastic simulations.

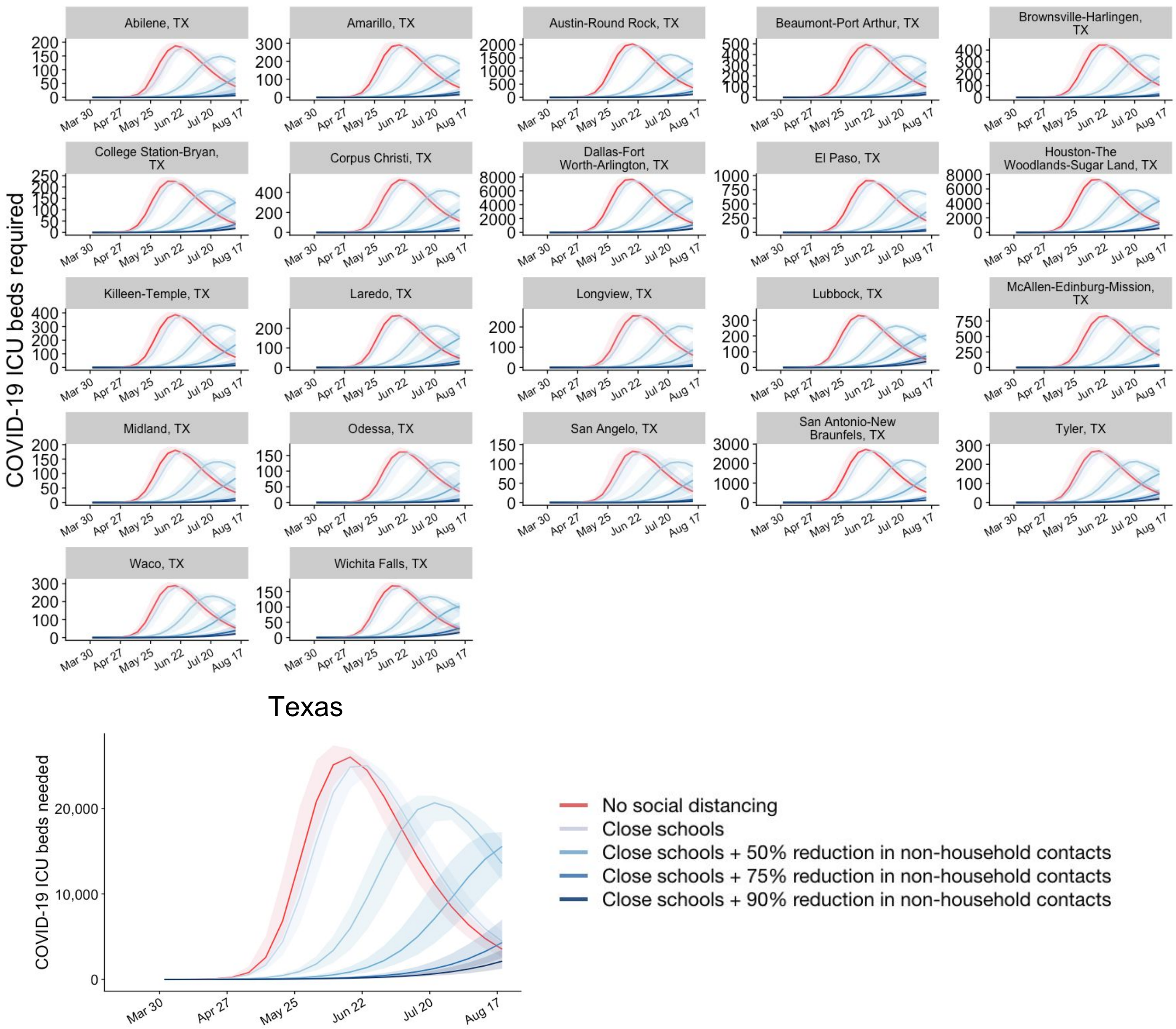

Figure 3. Projected COVID-19 cases requiring ICU treatment in 22 Texas metro/cities and summed across all 22 cities (bottom graph) under school closures from April 1 to August 17, 2020 coupled with different degrees of social distancing (starting from reported case counts on April 1). The red lines project COVID-19 transmission assuming no interventions. The blue lines show increasing levels of social distancing interventions, from light to dark: school closures plus social distancing interventions that reduce non-household contacts by either 50%, 75% or 90%. Lines and shading indicate the median value and interquartile range across 100 stochastic simulations.

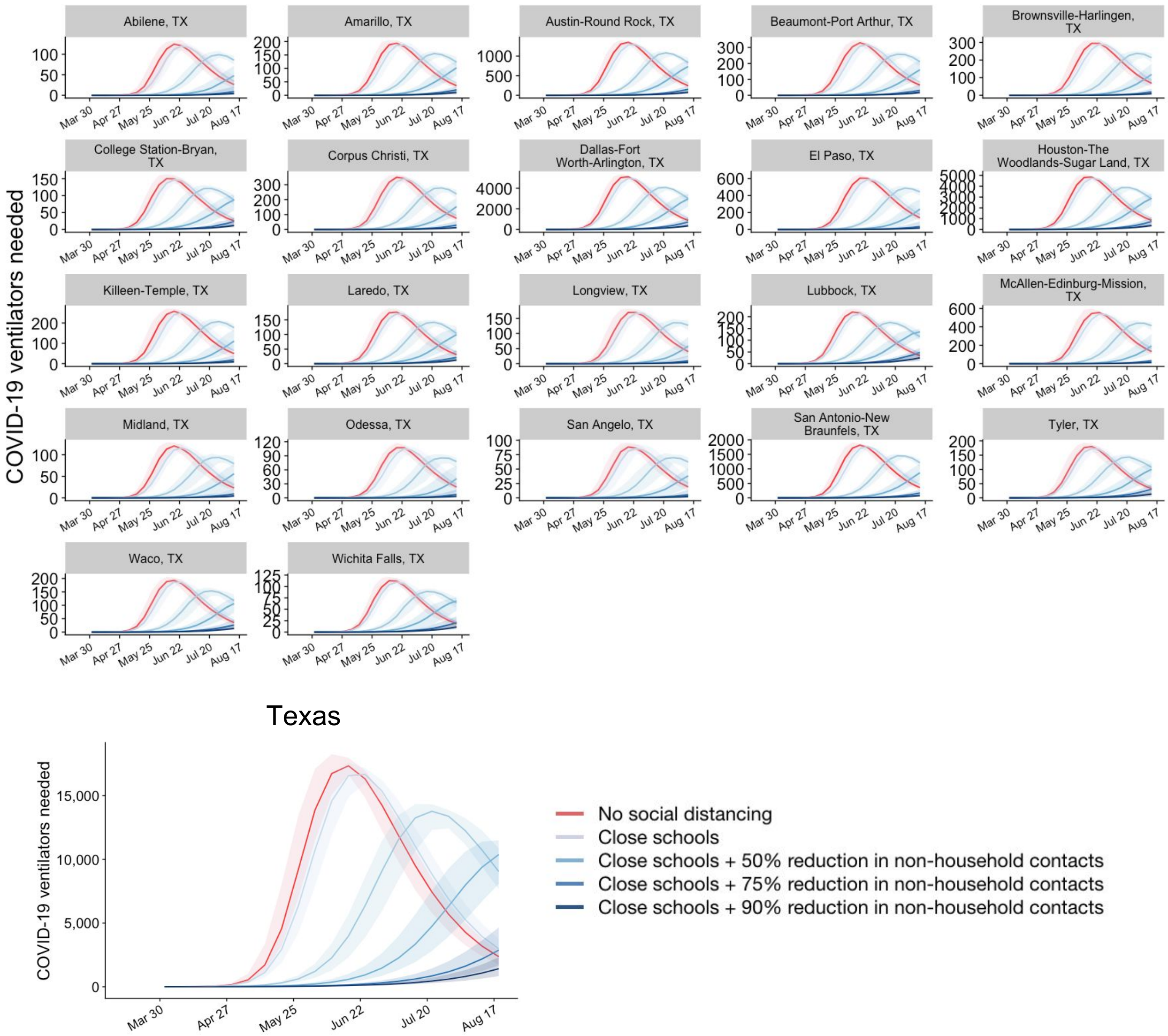

Figure 4. Projected COVID-19 patients requiring mechanical ventilation in 22 Texas metro/cities and summed across all 22 cities (bottom graph) under school closures from April 1 to August 17, 2020 coupled with different degrees of social distancing (starting from reported case counts on April 1). The red lines project COVID-19 transmission assuming no interventions. The blue lines show increasing levels of social distancing interventions, from light to dark: school closures plus social distancing interventions that reduce non-household contacts by either 50%, 75% or 90%. Lines and shading indicate the median value and interquartile range across 100 stochastic simulations.

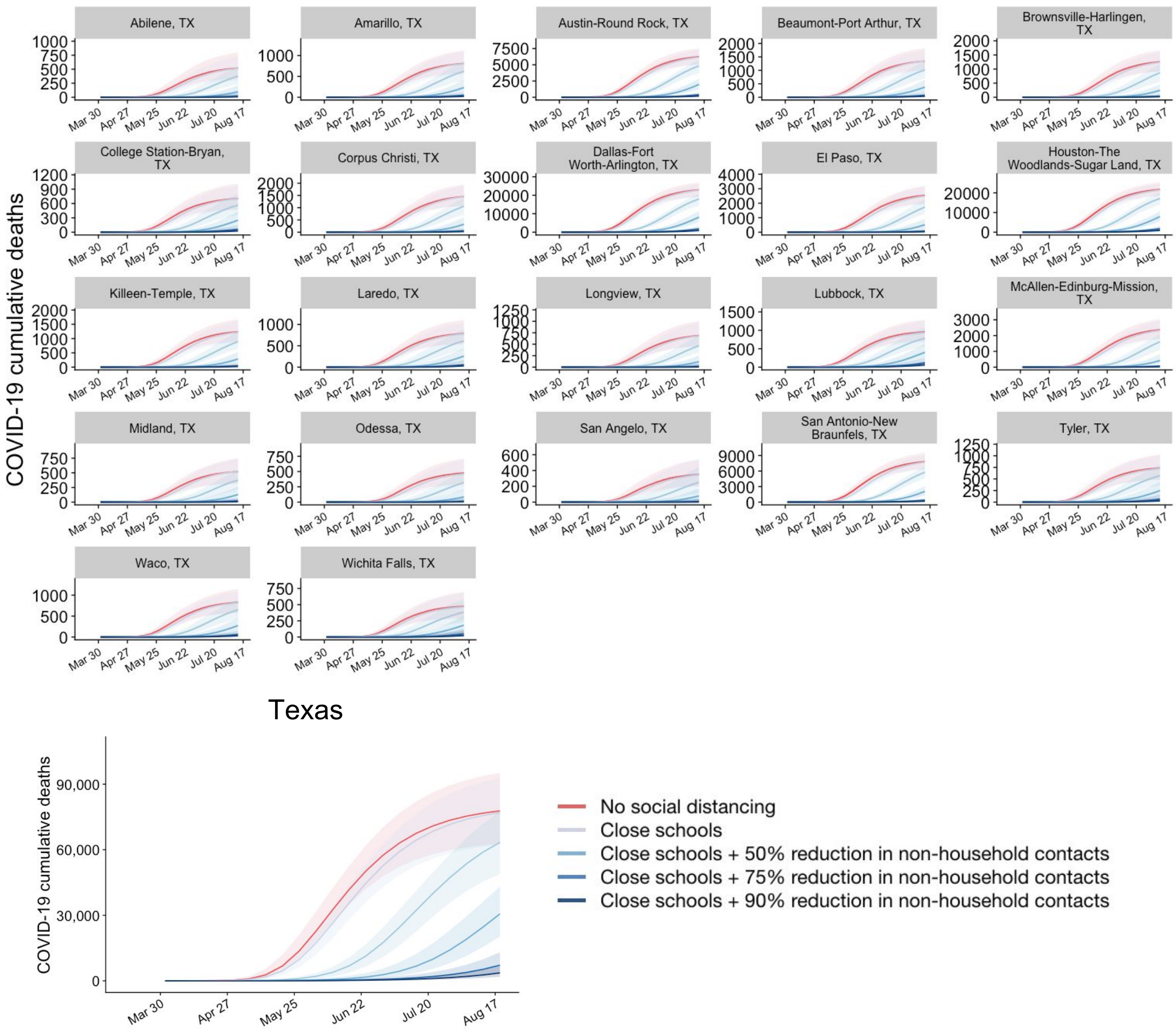

Figure 5. Projected COVID-19 cumulative deaths in 22 Texas metro/cities and summed across all 22 cities (bottom graph) under school closures from April 1 to August 17, 2020 coupled with different degrees of social distancing (starting from reported case counts on April 1). The red lines project COVID-19 transmission assuming no interventions. The blue lines show increasing levels of social distancing interventions, from light to dark: school closures plus social distancing interventions that reduce non-household contacts by either 50%, 75% or 90%. Lines and shading indicate the median value and interquartile range across 100 stochastic simulations.

Table 1. Projected COVID-19 cases, healthcare requirements and deaths summed across the 22 Texas cities from April 1 through August 17, 2020. The values are medians (and full min to max range) across 100 stochastic simulations based on the parameters given in the Appendix.

Outcomes	No measures	School closure	School closure + 50% social distancing	School closure + 75% social distancing	School closure + 90% social distancing	School closure + 95% social distancing
Cumulative cases	20,783,100 (14,180,526-27,784,228)	20,780,357 (15,100,908-26,673,881)	19,879,283 (13,786,595-26,173,365)	14,242,782 (9,606,298-18,668,719)	4,109,360 (2,371,804-6,629,406)	2,100,494 (1,234,482-3,342,599)
Peak incident cases (weekly)	5,020,8753 (4,243,105-5,715,942)	4,435,890 (3,850,399-4,963,025)	3,051,279 (2,558,265-3,319,696)	2,076,521 (1,649,027-2,342,677)	989,626 (579,333-144,9391)	504,909 (285,543-795,816)
Peak hospitalizations	216,953 (208,266-227,903)	208,656 (199,686-220,124)	172,284 (155,822-179,170)	117,072 (83,562-142,465)	27,198 (15,457-45,367)	13,404 (8,046-21,823)
Peak ICU	25,999 (24,955-27,368)	24,985 (23,916-26,412)	20,653 (18,637-21,486)	14,073 (10,063-17,088)	3,275 (1,860-5,458)	1,615 (966-2,626)
Peak Ventilators	17,333 (16,637-18,245)	16,657 (15,944-17,608)	13,769 (12,425-14,324)	9,382 (6,708-11,392)	2,183 (1,240-3,639)	1,076 (644-1,751)
Cumulative deaths	76,759 (62,072 -93,779)	75,702 (61,395-91,033)	58,954 (45,496-71,988)	24,667 (15,583-36,185)	5,285 (2,652-9,865)	2,713 (1,345-5,205)

Adjusted case (10% detection rate)

Figures 6-10 and Table 2 project COVID-19 cases, hospitalizations, ICU patients, ventilator requirements and deaths assuming that the number of people infected is equal to *ten times the total number of confirmed reported* cases in each city/MSA as of April 1 ([Table A2.1]).

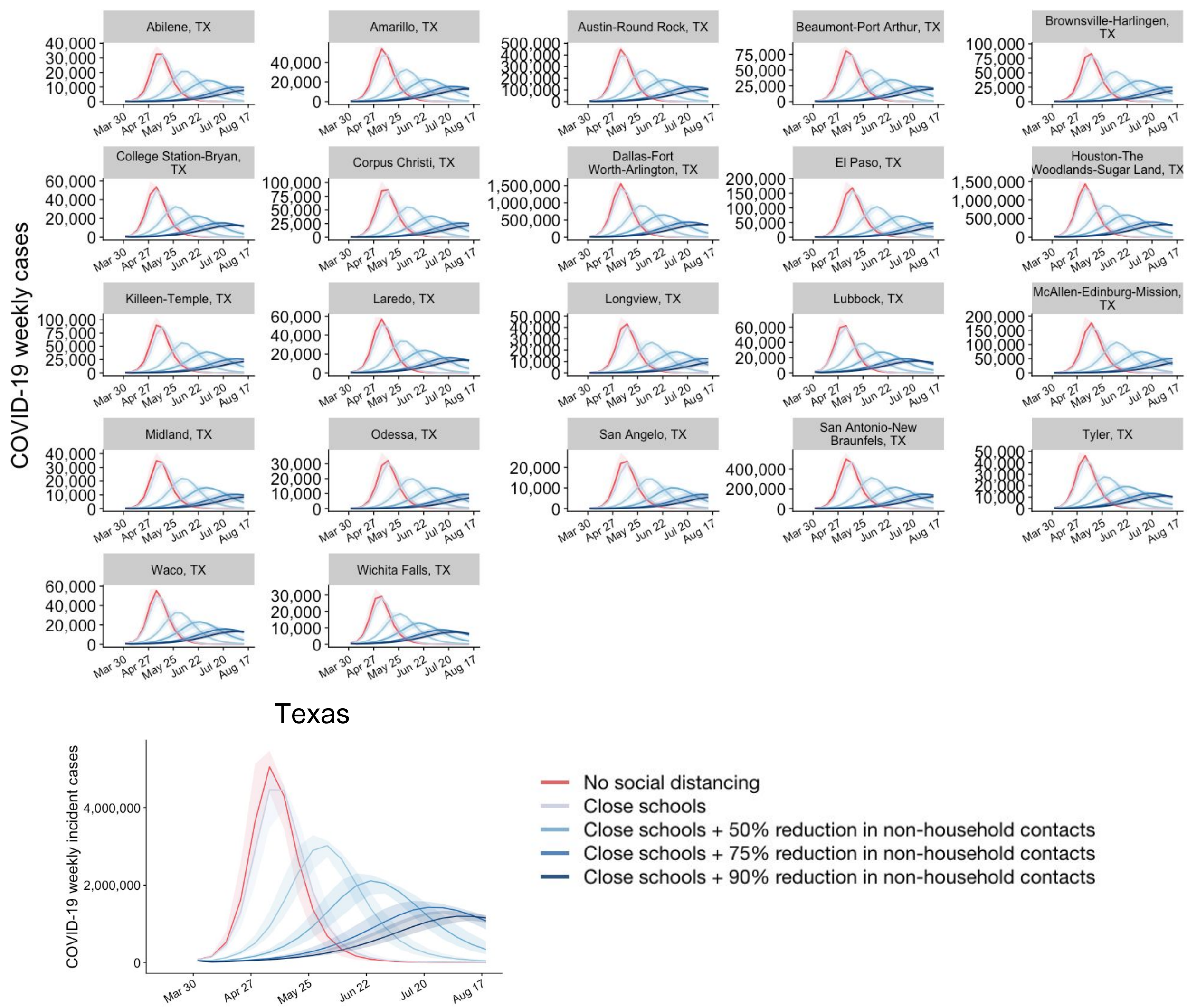

Figure 6. Projected new COVID-19 cases each week in 22 Texas metro/cities and summed across all 22 cities (bottom graph) under school closures from April 1 to August 17, 2020 coupled with different degrees of social distancing (assuming <10% case reporting rate). The red lines project COVID-19 transmission assuming no interventions. The blue lines show increasing levels of social distancing interventions, from light to dark: school closures plus social distancing interventions that reduce non-household contacts by either 50%, 75% or 90%. Lines and shading indicate the median value and interquartile range across 100 stochastic simulations.

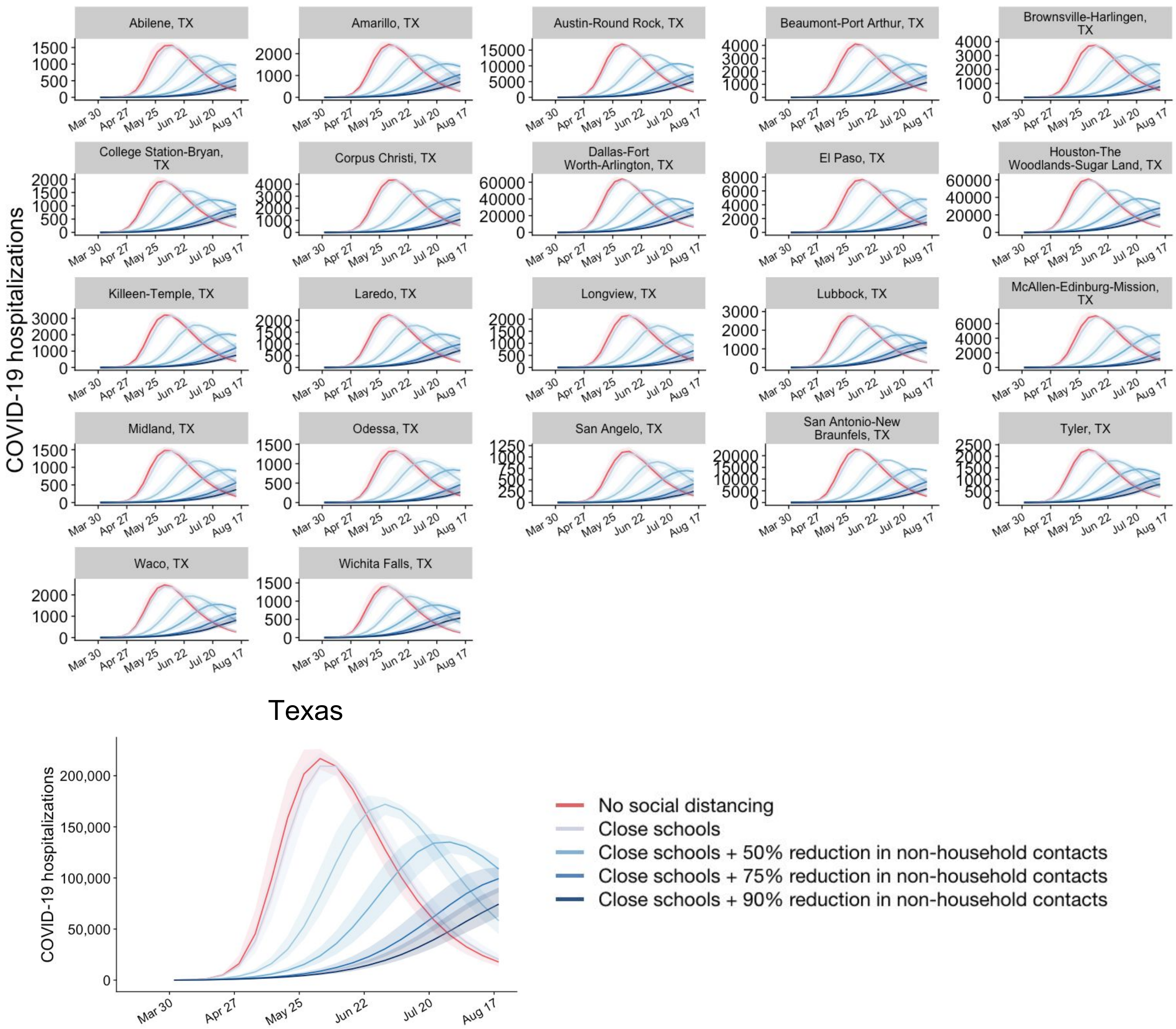

Figure 7. Projected COVID-19 hospitalizations in 22 Texas metro/cities and summed across all 22 cities (bottom graph) under school closures from April 1 to August 17, 2020 coupled with different degrees of social distancing (assuming <10% case reporting rate). The red lines project COVID-19 transmission assuming no interventions. The blue lines show increasing levels of social distancing interventions, from light to dark: school closures plus social distancing interventions that reduce non-household contacts by either 50%, 75% or 90%. Lines and shading indicate the median value and interquartile range across 100 stochastic simulations.

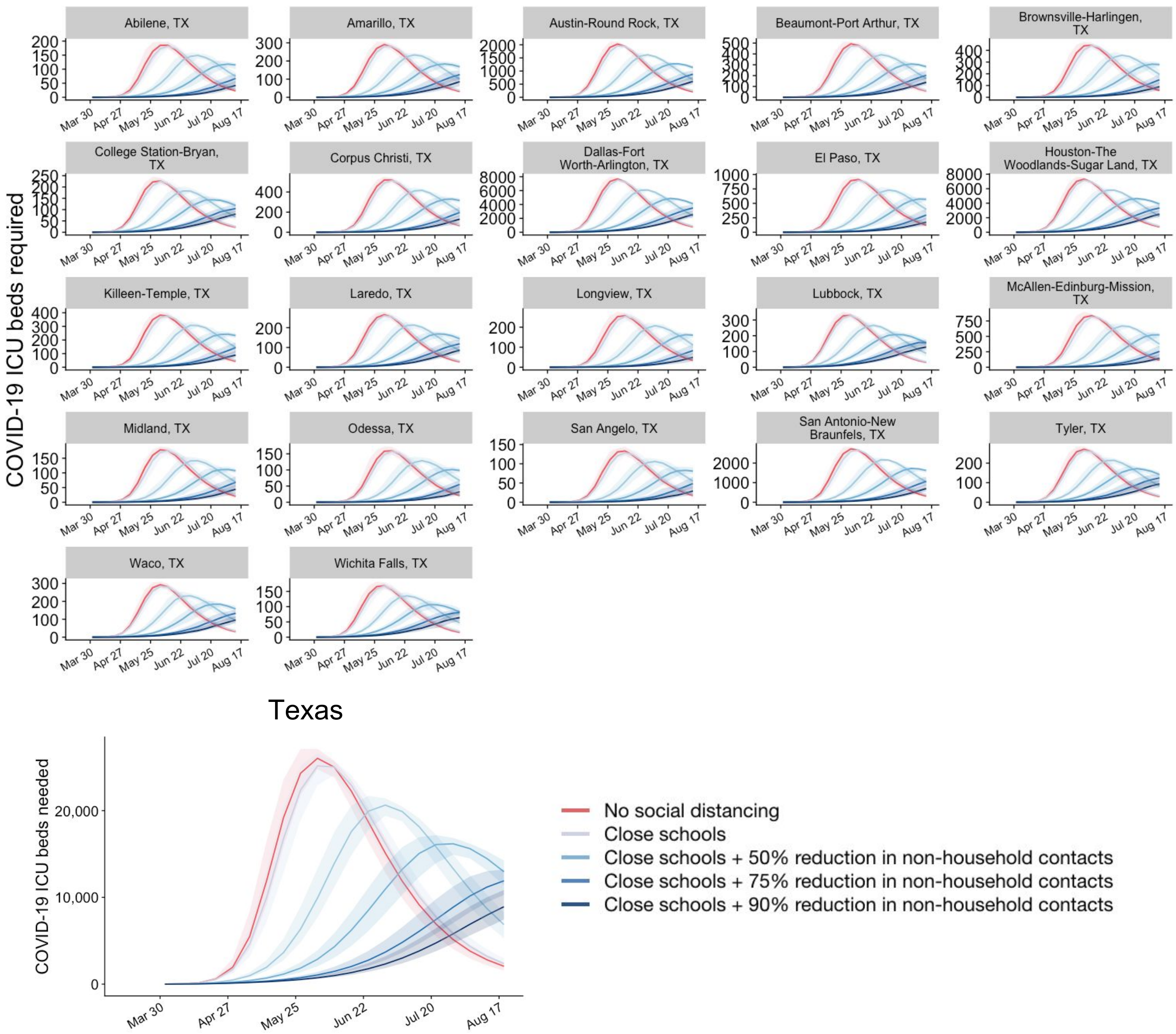

Figure 8. Projected COVID-19 cases requiring ICU treatment in 22 Texas metro/cities and summed across all 22 cities (bottom graph) under school closures from April 1 to August 17, 2020 coupled with different degrees of social distancing (assuming <10% case reporting rate). The red lines project COVID-19 transmission assuming no interventions. The blue lines show increasing levels of social distancing interventions, from light to dark: school closures plus social distancing interventions that reduce non-household contacts by either 50%, 75% or 90%. Lines and shading indicate the median value and interquartile range across 100 stochastic simulations.

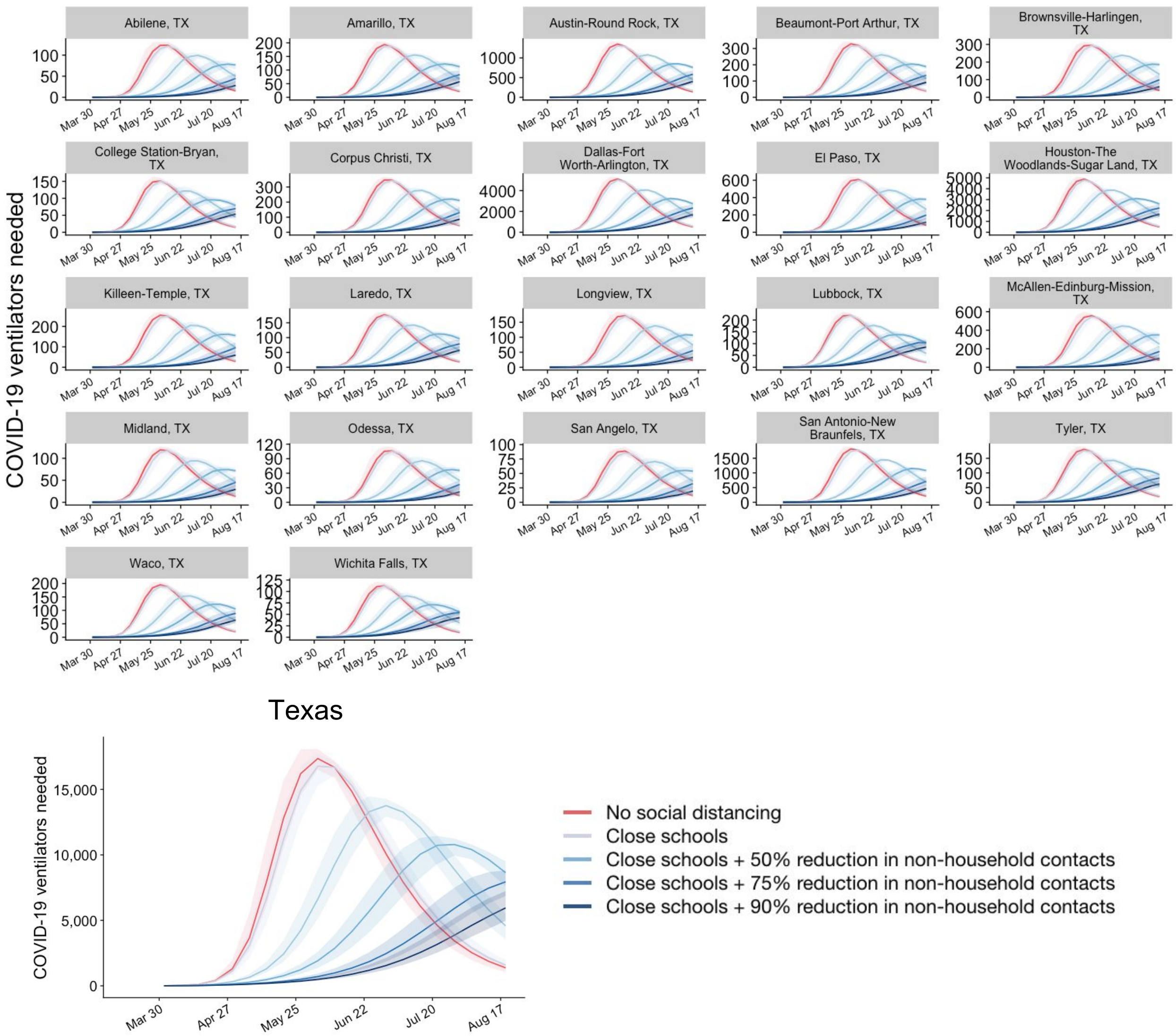

Figure 9. Projected COVID-19 patients requiring mechanical ventilation in 22 Texas metro/cities and summed across all 22 cities (bottom graph) under school closures from April 1 to August 17, 2020 coupled with different degrees of social distancing (assuming <10% case reporting rate). The red lines project COVID-19 transmission assuming no interventions. The blue lines show increasing levels of social distancing interventions, from light to dark: school closures plus social distancing interventions that reduce non-household contacts by either 50%, 75% or 90%. Lines and shading indicate the median value and interquartile range across 100 stochastic simulations.

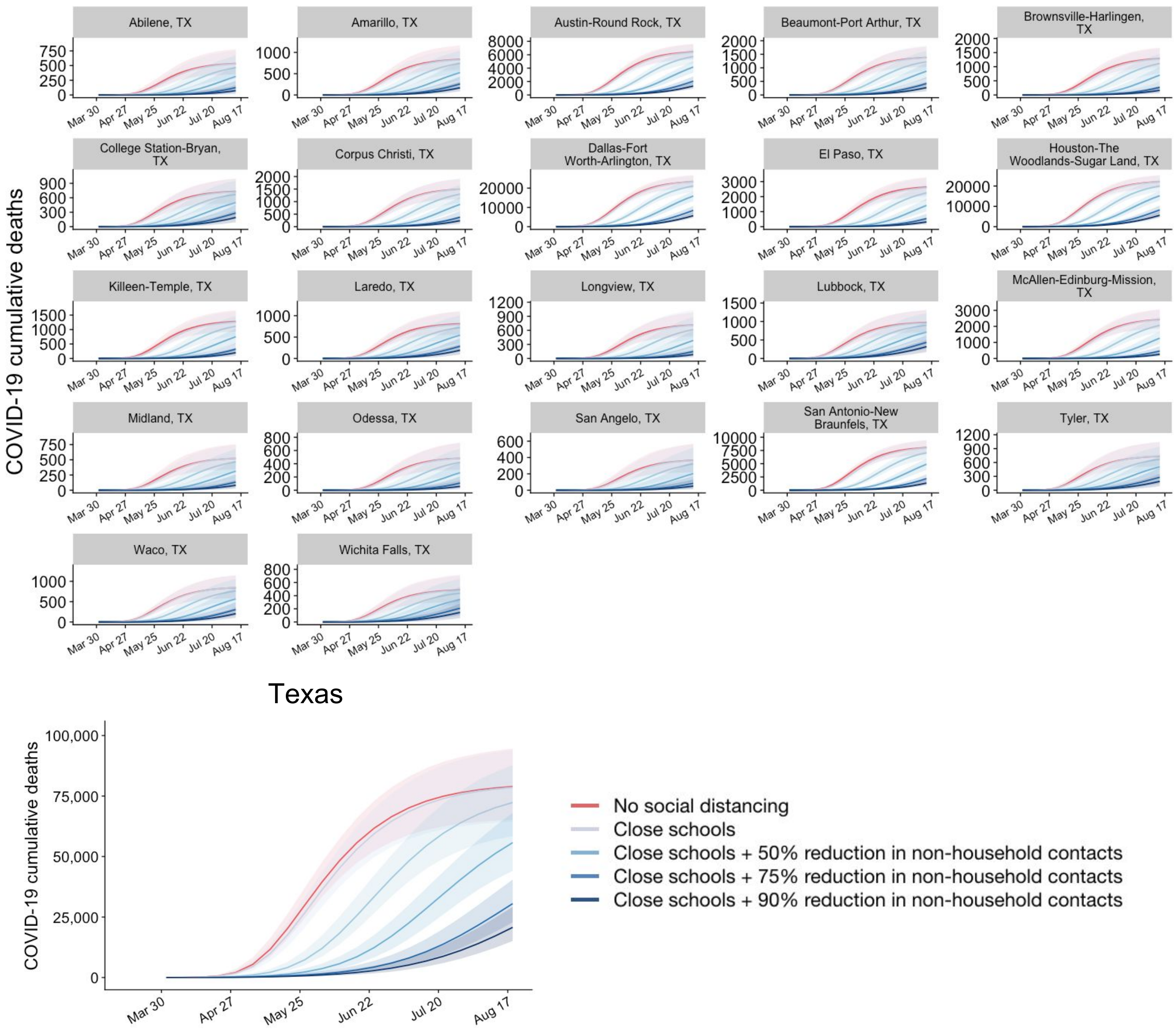

Figure 10. Projected COVID-19 cumulative deaths in 22 Texas metro/cities and summed across all 22 cities (bottom graph) under school closures from April 1 to August 17, 2020 coupled with different degrees of social distancing (assuming <10% case reporting rate). The red lines project COVID-19 transmission assuming no interventions. The blue lines show increasing levels of social distancing interventions, from light to dark: school closures plus social distancing interventions that reduce non-household contacts by either 50%, 75% or 90%. Lines and shading indicate the median value and interquartile range across 100 stochastic simulations.

Table 1. Projected COVID-19 cases, healthcare requirements and deaths summed across the 22 Texas cities from April 1 through August 17, 2020, assuming less than 10% of cases are reported. The values are medians (and full min to max range) across 100 stochastic simulations based on the parameters given in the Appendix.

Outcomes	No measures	School closure	School closure + 50% social distancing	School closure + 75% social distancing	School closure + 90% social distancing	School closure + 95% social distancing
Cumulative cases	20,809,025 (15,514,209-26,229,169)	20,797,426 (15,708,741-26,022,194)	20,281,814 (15,702,306-24,936,607)	18,383,688 (13,968,020-22,431,689)	12,554,748 (10,294,905-15,164,443)	9,259,252 (7,683,962-11,516,848)
Peak incident cases (weekly)	5,054,037 (4,389,447-5,468,342)	4,460,975 (3,927,990-5,108,091)	3020565 (2,720,067-3,292,486)	2,111,843 (1,787,236-2,302,058)	1,428,121 (1,276,034-1,594,399)	1,197,777 (1,084,557-1,336,978)
Peak hospitalizations	216,888 (206,042-226,249)	209,502 (201,312-222,092)	172,090 (161,758-180,858)	135,070 (124,305-143,369)	93,198 (78,440-108,713)	66,210 (54,290-83,418)
Peak ICU	26,034 (24,772-27,131)	25,157 (24,083-26,640)	20,638 (19,409-21,703)	16,183 (14,917-17,172)	11,189 (9,422-13,021)	7,954 (6,523-10,016)
Peak Ventilators	17,356 (16,515-180,87)	16,771 (16,055-17,760)	13,758 (12,939-14,469)	10,789 (9,944-11,448)	7,459 (6,281-8,681)	5,302 (4,349-6,677)
Cumulative deaths	78,372 (64,858-93,767)	77,868 (64,005-93,066)	70,202 (57,088-84,972)	51,276 (40,511-62,705)	25,992 (18,916-35,237)	17,216 (12,336-24,762)

Appendix 1

Scenario specifications

Table A1.1 Initial conditions, school closures and social distancing policies

Variable	**Settings**
Initial day of simulation	4/1/2020
Initial infection number in locations	Table A2.1
Trigger to close school	4/1/2020
Closure Duration	Until start of 2020-2021 school year (8/17/20)
α: Reduction of non-household contacts (work and other)	Five scenarios: 0%, 50%, 75%, 90%, 95%
Age-specific and day-specific contact rates	Home, work, other and school matrices provided in Tables A1.3-A1.6 Normal weekday = home + work + other + school Normal weekend = home + other Normal weekday holiday = home + other Normal weekday during summer or winter break = home + work + other School closure weekday = home + (1-α)*(work + other) School closure weekend = home + (1-α)*(other) School closure weekday holiday = home + (1-α)*(other) School closure during summer or winter break = home + (1-α)*(work + other)

Table A1.2 Model parameters. Values given as five-element vectors are age-stratified with values corresponding to 0-4, 5-17, 18-49, 50-64, 65+ year age groups, respectively.

Parameters	**Best guess values**	**Source**
R_0	2.2	[1]

δ: doubling time	4 days	[2]
Λ: growth rate	0.1733	$\Lambda = \frac{\ln(2)}{\delta}$
Serial interval	6.92 days	$\frac{R_0 - 1}{\Lambda}$
β: transmission rate	0.0260	Fitted to obtain specified R_0 given δ
γ_A: recovery rate on asymptomatic compartment	Equal to γ_Y	
γ_Y: recovery rate on symptomatic non-treated compartment	$\frac{1}{\gamma_Y} \sim \text{Triangular}(21.2, 22.6, 24.4)$	[5]
τ: symptomatic proportion (%)	82.1	[4]
σ: exposed rate	$\frac{1}{\sigma} \sim \text{Triangular}(5.6, 7, 8.2)$	[3]
P: proportion of pre-symptomatic (%)	12.6	[6]
ω_E: relative infectiousness of infectious individuals in compartment E	$\omega_E = \frac{(\frac{YHR}{\eta} + \frac{1-YHR}{\gamma_Y})\omega_Y \sigma P}{1-P}$	
ω_A: relative infectiousness of infectious individuals in compartment I^A	0.4653	Set to mean of ω_E

IFR: infected fatality ratio, age specific (%)	Low risk: [0.00091668, 0.0021789, 0.03388 , 0.25197, 0.64402] High risk: [0.009167, 0.02179, 0.33878, 2.5197, 6.4402]	Age adjusted from [5]
h: high-risk proportion, age specific (%)	[8.2825, 14.1121, 16.5298, 32.9912, 47.0568]	CDC
rr: relative risk for high risk people compared to low risk in their age group	10	Assumption
School calendar	2019-2020 and 2020-2019 calendar of school days	Calendar largest public school district in each metropolitan area/city [7]
Hospitalization Parameters		
γ_H: recovery rate in hospitalized compartment	1/14	14 day-average from admission to discharge (UT Austin Dell Med)
YHR: symptomatic case hospitalization rate (%)	Low risk: [0.0279, 0.0215, 1.3215, 2.8563, 3.3873] High risk: [0.2791, 0.2146, 13.2154, 28.5634, 33.8733]	Age adjusted from [5]
π: rate of symptomatic individuals go to hospital, age-specific	$\pi = \frac{\gamma_Y * YHR}{\eta + (\gamma_Y - \eta)YHR}$	
η: rate from symptom onset to hospitalized	0.1695	5.9 day average from symptom onset to hospital admission [8]
μ: rate from hospitalized to death	1/14	14 day-average from admission to death (UT Austin Dell Med)
HFR: hospitalized fatality ratio, age specific (%)	[4, 12.365, 3.122, 10.745, 23.158]	$HFR = \frac{IFR}{YHR(1-\tau)}$

ν: death rate on hospitalized individuals, age specific	[0.0390, 0.1208, 0.0304, 0.1049, 0.2269]	$\nu = \frac{\gamma_H HFR}{\mu + (\gamma_H - \mu)HFR}$
ICU: proportion hospitalized people in ICU	[0.15, 0.20, 0.15, 0.20, 0.15]	CDC planning scenarios (based on US seasonal flu data)
Vent: proportion of individuals in ICU needing ventilation	[0.67, 0.67, 0.67, 0.67, 0.67]	Assumption
d_{ICU} : duration of stay in ICU	10 days	Assumption, set equal to duration of ventilation
d_V : duration of ventilation	10 days	Assumption

Table A1.3 Home contact matrix. Daily number contacts by age group at home.

	0-4y	**5-17y**	**18-49y**	**50-64y**	**65y+**
0-4y	0.5	0.9	2.0	0.1	0.0
5-17y	0.2	1.7	1.9	0.2	0.0
18-49y	0.2	0.9	1.7	0.2	0.0
50-64y	0.2	0.7	1.2	1.0	0.1
65y+	0.1	0.7	1.0	0.3	0.6

Table A1.4 School contact matrix. Daily number contacts by age group at school.

	0-4y	**5-17y**	**18-49y**	**50-64y**	**65y+**
0-4y	1.0	0.5	0.4	0.1	0.0
5-17y	0.2	3.7	0.9	0.1	0.0
18-49y	0.0	0.7	0.8	0.0	0.0
50-64y	0.1	0.8	0.5	0.1	0.0
65y+	0.0	0.0	0.1	0.0	0.0

Table A1.5 Work contact matrix. Daily number contacts by age group at work.

	0-4y	5-17y	18-49y	50-64y	65y+
0-4y	0.0	0.0	0.0	0.0	0.0
5-17y	0.0	0.1	0.4	0.0	0.0
18-49y	0.0	0.2	4.5	0.8	0.0
50-64y	0.0	0.1	2.8	0.9	0.0
65y+	0.0	0.0	0.1	0.0	0.0

Table A1.6 Others contact matrix. Daily number contacts by age group at other locations.

	0-4y	5-17y	18-49y	50-64y	65y+
0-4y	0.7	0.7	1.8	0.6	0.3
5-17y	0.2	2.6	2.1	0.4	0.2
18-49y	0.1	0.7	3.3	0.6	0.2
50-64y	0.1	0.3	2.2	1.1	0.4
65y+	0.0	0.2	1.3	0.8	0.6

Appendix 2

Metapopulation model of COVID-19 Transmission in the US

The model consists of the following components, with links to data tables:

- Aggregation of 500 US cities into 217 populations (nodes) based on metropolitan and micropolitan designations and shared airports.
- Population structure within each of the 217 nodes:
  - Population sizes of 5 distinct age groups within each node (0-4, 5-17, 18-49, 50-64, and 65+) based on 2017 American Community Survey 5-Year Data [10].
- Mobility among the 217 nodes
  - Air travel: Node-to-node air travel based on 2018-2019 data from the US Bureau of Transportation Statistics [11]
  - Workflow: Node-to-node work-related ground travel based on 2011-2015 data from the US Census Bureau [12] for weekdays and weekends.
- School calendars are obtained from published school district calendars for 2019-2020 [7] and shifted for 2020-2021 based on Labor Day.
- Contact matrices (Tables A1.3-A1.6). Ref. [13] provides contact rates for the United States derived from population-based contact diaries in eight European countries from the POLYMOD study [14]. The original POLYMOD data was used to estimate age and location specific contact patterns, which were then extrapolated to other countries based on the similarity to the original countries using demographic and household structure information, as well as school participation and workforce enrollment. The rates are broken down by age group (0-4, 5-9, 10-14, 15-19, 20-24, 25-29, 30-34, 35-39, 40-44, 45-49, 50-54, 55-59, 60-64, 65-69, 70-75, 75+) and by type of contact (at home, work, school and other locations). Then each location specific contact matrix was aggregated into the 5 age groups used in our model, using US population in each of those age groups. We classify days into four categories and used these reported values to estimate the corresponding contact matrices as follows:
  - <u>Weekdays when school is in session</u>: All reported contacts

- ○ Weekdays during school holidays: All reported contacts except those occurring in school
- ○ Weekdays during school closures: All reported contacts except those occurring in school and a specified fraction of those occurring at work.
- ○ Weekends: All reported contacts except those occurring in school and work.

- Epidemiological dynamics. Disease transmission within and between nodes are governed by age- and risk-stratified SEIR models within each node that incorporate the school calendar and implement school closures as changes to age-specific contact rates (Figure A2.1).
  - ○ Subpopulations are defined by geographic node *i*, age group *a*, risk group *r*
  - ○ Each subpopulation is split into epidemiological compartments: susceptible, exposed, asymptomatic, symptomatic, hospitalized, recovered, and deceased.

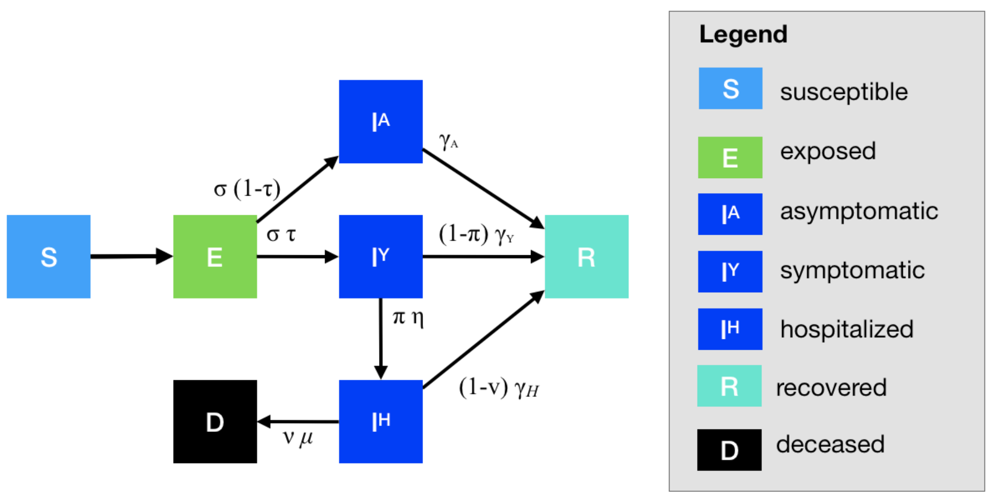

Figure A2.1. Diagram of within-node compartmental model. Each subgroup (defined by age class and risk group) is modeled with a separate set of compartments. Upon infection, susceptible individuals (S) progress to exposed (E) where they are pre-symptomatic and possibly infectious and then to either symptomatic infectious (I^Y) or asymptomatic infectious (I^A). All asymptomatic cases eventually progress to a recovered class where they remain permanently protected from future infection (R); symptomatic cases are either hospitalized (I^H) or recover. Influenza mortality (D) varies by population subgroup and is assumed to be preceded by hospitalization. We model stochastic transitions between compartments using the τ-leap method [80,81] with key parameters given in Table A1.2.

- Force of Infection.
    - The *within-node force of infection* for susceptible people in group of *i, a, r* is given by

$$\Upsilon_{i,a,r} = \sum_{g \in G} \sum_{k \in K} (E_{i,g,k}\omega_E + I^Y_{i,g,k}\omega_Y + I^A_{i,g,k}\omega_A)\beta_i \phi_{a,g}/N_{i,g}$$

      where *G* and *K* indicates all possible age groups and risk groups, respectively. All other variable and parameter symbols are defined in Table A1.2.

    - The *between-node transmission of disease* assumes that symptomatic individuals do not travel. The *between-node force of infection* for susceptible people in group of *i, a, r* is then given by

$$\lambda_{i,a,r} = \sum_{j \neq i} \sum_{g \in G} \sum_{k \in K} \zeta_{i,j,a}(E_{j,g,k}\omega_E + I^Y_{j,g,k}\omega_Y + I^A_{j,g,k}\omega_A)\beta_j \phi_{a,g}/N_{j,g}$$

$$+ \sum_{j \neq i} \sum_{g \in G} \sum_{k \in K} \zeta_{j,i,g}(E_{j,g,k}\omega_{gC} + I^A_{j,g,k}\omega_Y)\beta_i \phi_{a,g}/N_{i,g}$$

with the variable and parameter symbols as defined in Table A1.2. The first term corresponds to the susceptible individual becoming infected while visiting another city; the second term corresponds to the susceptible individual becoming infected in his/her home node through exposure to an infected traveler visiting from another city.

Texas Component of US COVID-19 Pandemic Model

The projections in this report are based on simulations for the 22 largest cities/metros in Texas within our *US COVID-19 Pandemic Model* (Table A1.2 and Figure A2.2). These 22 populations comprise about 43% of the Texas population and 12% of its geographic expanse. Each city/metro model includes local estimates for age distribution and proportion of each age group that is high risk (for example, Figure A2.3).

Table A2.2. Reported COVID-19 cases as of April 1, 2020 and population sizes for the 22 Texas cities/metros included in the *US COVID-19 Pandemic Model*. For cities reporting zero cases, the simulations were initialized assuming that one adult was infected on April 1, 2020.

For several of the large metropolitan areas, the population sizes do not cover the entire MSA rather they are the sum of all cities within the MSA included in the CDC's 500 Cities Project [15].

CBSA Code	City/Metro	Cumulative reported cases	Population
19100	Dallas-Fort Worth-Arlington, TX	1,365	7,599,553
26420	Houston-The Woodlands-Sugar Land, TX	1,351	7,058,699
41700	San Antonio-New Braunfels, TX	253	2,537,904
12420	Austin-Round Rock, TX	346	2,185,876
47380	McAllen-Edinburg-Mission, TX	46	873,872
46340	El Paso, TX	50	852,474
21340	Killeen-Temple, TX	45	457,168
31180	Corpus Christi, TX	38	456,155
48660	Brownsville-Harlingen, TX	26	427,321
17780	Beaumont-Port Arthur, TX	47	412,693
28660	Lubbock, TX	100	321,300
30980	Laredo, TX	45	278,595
15180	Waco, TX	48	273,785
29700	Amarillo, TX	33	268,024
36220	College Station-Bryan, TX	66	263,985
10180	Tyler, TX	43	232,037
11100	Longview, TX	13	221,102
13140	Midland, TX	16	180,104
18580	Abilene, TX	14	172,646
32580	Odessa, TX	11	163,687
33260	Wichita Falls, TX	39	152,300
41660	San Angelo, TX	9	120,576

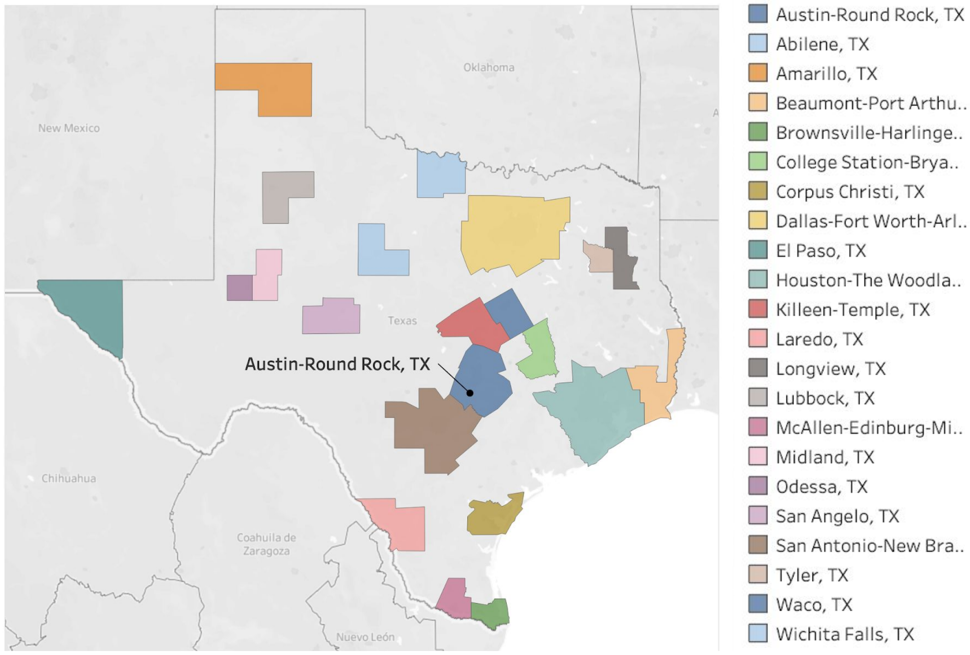

Figure A2.2. Texas cities and metropolitan areas included in the US COVID-19 Pandemic Model.

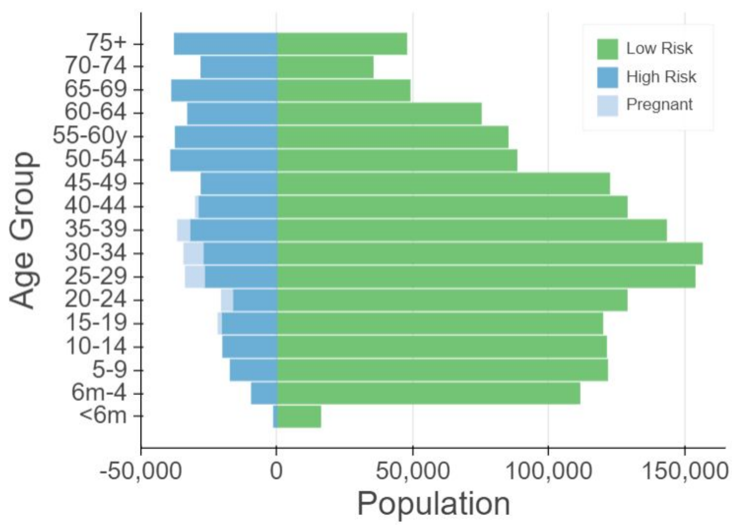

Figure A2.3. Demographic and risk composition of the Austin-Round Rock population. Bars indicate age-specific population sizes, separated by low risk, high risk, and pregnant. High risk is defined as individuals with cancer, chronic kidney disease, COPD, heart disease, stroke asthma, diabetes, HIV/AIDS, and morbid obesity, as estimated from the CDC 500 Cities Project [15], reported HIV prevalence [16] and reported morbid obesity prevalence [17,18], corrected for multiple conditions. The population of pregnant women is derived using the CDC's method combining fertility, abortion and fetal loss rates [19–21]. Each of the 22 city models includes similar local estimates for age and risk group proportions.

References

1. Li Q, Guan X, Wu P, Wang X, Zhou L, Tong Y, et al. Early Transmission Dynamics in Wuhan, China, of Novel Coronavirus-Infected Pneumonia. N Engl J Med. 2020. doi:10.1056/NEJMoa2001316

2. Kraemer MUG, Yang C-H, Gutierrez B, Wu C-H, Klein B, Pigott DM, et al. The effect of human mobility and control measures on the COVID-19 epidemic in China. medRxiv. 2020. Available: https://www.medrxiv.org/content/10.1101/2020.03.02.20026708v1

3. Lauer SA, Grantz KH, Bi Q, Jones FK, Zheng Q, Meredith HR, et al. The Incubation Period of Coronavirus Disease 2019 (COVID-19) From Publicly Reported Confirmed Cases: Estimation and Application. Ann Intern Med. 2020. doi:10.7326/M20-0504

4. Mizumoto K, Kagaya K, Zarebski A, Chowell G. Estimating the Asymptomatic Proportion of 2019 Novel Coronavirus onboard the Princess Cruises Ship, 2020. Infectious Diseases (except HIV/AIDS). medRxiv; 2020. doi:10.1101/2020.02.20.20025866

5. Verity R, Okell LC, Dorigatti I, Winskill P, Whittaker C, Imai N, et al. Estimates of the severity of COVID-19 disease. Epidemiology. medRxiv; 2020. doi:10.1101/2020.03.09.20033357

6. Du Z, Xu X, Wu Y, Wang L, Cowling BJ, Meyers LA. The serial interval of COVID-19 from publicly reported confirmed cases. Epidemiology. medRxiv; 2020. doi:10.1101/2020.02.19.20025452

7. United States School Calendar 2020 - PublicHolidays.us. In: PublicHolidays.us [Internet]. [cited 1 Mar 2020]. Available: https://publicholidays.us/school-holidays/

8. Tindale L, Coombe M, Stockdale JE, Garlock E, Lau WYV, Saraswat M, et al. Transmission interval estimates suggest pre-symptomatic spread of COVID-19. Epidemiology. medRxiv; 2020. doi:10.1101/2020.03.03.20029983

9. Sanche S, Lin YT, Xu C, Romero-Severson E, Hengartner N, Ke R. The Novel Coronavirus, 2019-nCoV, is Highly Contagious and More Infectious Than Initially Estimated. Epidemiology. medRxiv; 2020. doi:10.1101/2020.02.07.20021154

10. US Census Bureau. American Community Survey (ACS). [cited 19 Nov 2019]. Available: https://www.census.gov/programs-surveys/acs

11. OST_R | BTS | Transtats. [cited 31 Jan 2020]. Available: https://www.transtats.bts.gov/tables.asp?Table_ID=288&SYS_Table_Name=T_MASTER_CORD

12. US Census Bureau. 2011-2015 5-Year ACS Commuting Flows. [cited 21 Jan 2020]. Available:

https://www.census.gov/data/tables/2015/demo/metro-micro/commuting-flows-2015.html

13. Prem K, Cook AR, Jit M. Projecting social contact matrices in 152 countries using contact surveys and demographic data. PLoS Comput Biol. 2017;13: e1005697.

14. Mossong J, Hens N, Jit M, Beutels P, Auranen K, Mikolajczyk R, et al. Social contacts and mixing patterns relevant to the spread of infectious diseases. PLoS Med. 2008;5: e74.

15. 500 Cities Project: Local data for better health | Home page | CDC. 5 Dec 2019 [cited 19 Mar 2020]. Available: https://www.cdc.gov/500cities/index.htm

16. for Disease Control C, Prevention, Others. HIV surveillance report. 2016; 28. URL: http://www cdc gov/hiv/library/reports/hiv-surveil-lance html Published November. 2017.

17. Sturm R, Hattori A. Morbid obesity rates continue to rise rapidly in the United States. Int J Obes . 2013;37: 889–891.

18. Morgan OW, Bramley A, Fowlkes A, Freedman DS, Taylor TH, Gargiullo P, et al. Morbid obesity as a risk factor for hospitalization and death due to 2009 pandemic influenza A(H1N1) disease. PLoS One. 2010;5: e9694.

19. Martin JA, Hamilton BE, Osterman MJK, Driscoll AK, Drake P. Births: Final Data for 2017. Natl Vital Stat Rep. 2018;67: 1–50.

20. Jatlaoui TC, Boutot ME, Mandel MG, Whiteman MK, Ti A, Petersen E, et al. Abortion Surveillance - United States, 2015. MMWR Surveill Summ. 2018;67: 1–45.

21. Ventura SJ, Curtin SC, Abma JC, Henshaw SK. Estimated pregnancy rates and rates of pregnancy outcomes for the United States, 1990-2008. Natl Vital Stat Rep. 2012;60: 1–21.